



# Decadal trends in the ocean carbon sink

Tim DeVries<sup>a,b,1</sup>, Corinne Le Quéré<sup>c</sup>, Oliver Andrews<sup>c,d</sup>, Sarah Berthet<sup>e</sup>, Judith Hauck<sup>f</sup>, Tatiana Ilyina<sup>g</sup>, Peter Landschützer<sup>g</sup>, Andrew Lenton<sup>h,i,j</sup>, Ivan D. Lima<sup>k</sup>, Michael Nowicki<sup>a,b</sup>, Jörg Schwinger<sup>l</sup>, and Roland Séférian<sup>e</sup>

<sup>a</sup>Department of Geography, University of California, Santa Barbara, CA 93106; <sup>b</sup>Earth Research Institute, University of California, Santa Barbara, CA 93106;

<sup>c</sup>Tyndall Centre for Climate Change Research, School of Environmental Sciences, University of East Anglia, Norwich NR4 7TJ, United Kingdom; <sup>d</sup>School of Geographical Sciences, University of Bristol, Bristol BS8 1TH, United Kingdom; <sup>e</sup>Centre National de Recherche Météorologique, Unité Mixte de Recherche, 31100 Toulouse, France; <sup>f</sup>Alfred-Wegener-Institut-Helmholtz-Zentrum für Polar und Meeresforschung, 27570 Bremerhaven, Germany; <sup>g</sup>Max Planck Institute for Meteorology, 20146 Hamburg, Germany; <sup>h</sup>Oceans and Atmosphere, Commonwealth Scientific and Industrial Research Organisation (CSIRO), Hobart, Battery Point, TAS 7004, Australia; <sup>i</sup>Centre for Southern Hemisphere Oceans Research, CSIRO Marine Laboratories, Hobart, TAS 7000, Australia;

<sup>j</sup>Antarctic Climate and Ecosystems Cooperative Research Centre, Hobart, TAS 7001, Australia; <sup>k</sup>Department of Marine Chemistry and Geochemistry, Woods Hole Oceanographic Institution, Woods Hole, MA 02543; and <sup>l</sup>NORCE Norwegian Research Centre, Bjerknes Centre for Climate Research, NO-5007 Bergen, Norway

Edited by David M. Karl, University of Hawaii, Honolulu, HI, and approved April 26, 2019 (received for review January 10, 2019)

**Measurements show large decadal variability in the rate of CO<sub>2</sub> accumulation in the atmosphere that is not driven by CO<sub>2</sub> emissions. The decade of the 1990s experienced enhanced carbon accumulation in the atmosphere relative to emissions, while in the 2000s, the atmospheric growth rate slowed, even though emissions grew rapidly. These variations are driven by natural sources and sinks of CO<sub>2</sub> due to the ocean and the terrestrial biosphere. In this study, we compare three independent methods for estimating oceanic CO<sub>2</sub> uptake and find that the ocean carbon sink could be responsible for up to 40% of the observed decadal variability in atmospheric CO<sub>2</sub> accumulation. Data-based estimates of the ocean carbon sink from pCO<sub>2</sub> mapping methods and decadal ocean inverse models generally agree on the magnitude and sign of decadal variability in the ocean CO<sub>2</sub> sink at both global and regional scales. Simulations with ocean biogeochemical models confirm that climate variability drove the observed decadal trends in ocean CO<sub>2</sub> uptake, but also demonstrate that the sensitivity of ocean CO<sub>2</sub> uptake to climate variability may be too weak in models. Furthermore, all estimates point toward coherent decadal variability in the oceanic and terrestrial CO<sub>2</sub> sinks, and this variability is not well-matched by current global vegetation models. Reconciling these differences will help to constrain the sensitivity of oceanic and terrestrial CO<sub>2</sub> uptake to climate variability and lead to improved climate projections and decadal climate predictions.**

carbon dioxide | ocean carbon sink | terrestrial carbon sink | climate variability | carbon budget

**A**nthropogenic emissions of carbon dioxide (CO<sub>2</sub>) are a major contributor to climate change, accounting for >80% of the radiative forcing of anthropogenic greenhouse gases over the past several decades (1). There is therefore a pressing need to understand the factors influencing the rate at which anthropogenic CO<sub>2</sub> accumulates in the atmosphere. The primary driver of atmospheric CO<sub>2</sub> accumulation is anthropogenic emissions from industrial activity and deforestation (2), which has increased by ~60% over the past 30 y (Fig. 1A). CO<sub>2</sub> accumulation in the atmosphere, however, has not always followed the trend in CO<sub>2</sub> emissions. From 1990 to 1999, atmospheric CO<sub>2</sub> accumulated more rapidly than expected from the relatively slow growth in emissions, while in the decade from 2000 to 2009, atmospheric CO<sub>2</sub> accumulation was relatively steady, while emissions rose rapidly (Fig. 1A).

This decadal variability in atmospheric CO<sub>2</sub> accumulation rate is linked to variability in the sources and sinks of CO<sub>2</sub> in the natural environment (5). The most important of these natural sources and sinks are terrestrial ecosystems and ocean waters. Other natural sources and sinks such as volcanoes and rock weathering are much smaller and change very slowly (6) and can be neglected on recent timescales. Thus, the global carbon budget (3) is primarily a balance between anthropogenic CO<sub>2</sub> emissions from fossil-fuel burning and cement manufacturing (FF) and land-use change

(LUC; i.e., deforestation), and changes in the accumulation of CO<sub>2</sub> in the atmosphere (C<sub>atm</sub>), ocean (C<sub>oce</sub>), and land biosphere (C<sub>land</sub>),

$$(FF+LUC) - \frac{dC_{atm}}{dt} - \frac{dC_{oce}}{dt} - \frac{dC_{land}}{dt} = 0. \quad [1]$$

Global FF and LUC emissions have an uncertainty of ~10% (3, 7, 8), and atmospheric CO<sub>2</sub> has been measured continuously since 1980 at a global network of stations, with error on the annual average accumulation of < 5% (9). From these observations and Eq. (1), we can infer the accumulation rate of carbon in the combined land and ocean reservoirs (Fig. 1A). The total rate of land+ocean carbon accumulation has averaged  $55 \pm 10\%$  of total carbon emissions over the past 30 y, but has shown significant decadal variability. The 1990s experienced a weakening of the land+ocean carbon sink, while the first decade of the 2000s was characterized by a strengthening land+ocean carbon sink (Fig. 1B).

The relative contribution of the land and ocean carbon sinks to this decadal variability cannot be directly measured, due to the heterogeneity of carbon accumulation and large natural carbon reservoirs. For this reason, dynamic global vegetation models (DGVMs) and global ocean biogeochemistry models

## Significance

**The ocean and land absorb anthropogenic CO<sub>2</sub> from industrial fossil-fuel emissions and land-use changes, helping to buffer climate change. Here, we compare decadal variability of ocean CO<sub>2</sub> uptake using three independent methods and find that the ocean could be responsible for as much as 40% of the observed decadal variability of CO<sub>2</sub> accumulation in the atmosphere. The remaining variability is due to variability in the accumulation of carbon in the terrestrial biosphere. Models capture these variations, but not as strongly as the observations, implying that CO<sub>2</sub> uptake by the land and ocean is more sensitive to climate variability than currently thought. Models must capture this sensitivity to provide accurate climate predictions.**

Author contributions: T.D. and C.L.Q. designed research; T.D., O.A., S.B., J.H., T.I., A.L., I.D.L., J.S., and R.S. performed research; T.D., and M.N. analyzed data; and T.D., C.L.Q., O.A., S.B., J.H., T.I., P.L., A.L., I.D.L., J.S., and R.S. wrote the paper.

The authors declare no conflict of interest.

This article is a PNAS Direct Submission.

Data deposition: OCIM data are available at <https://tdevries.eri.ucsb.edu/models-and-data-products/>. Timeseries of the SOCOM data following ref. 15 can be obtained from <http://www.bgc-jena.mpg.de/SOCOM/>. Timeseries of the GOBM data are available at <https://doi.org/10.6084/m9.figshare.8091161>.

Published under the PNAS license.

<sup>1</sup>To whom correspondence may be addressed. Email: tdevries@geog.ucsb.edu.

This article contains supporting information online at [www.pnas.org/lookup/suppl/doi:10.1073/pnas.1900371116/-DCSupplemental](https://www.pnas.org/lookup/suppl/doi:10.1073/pnas.1900371116/-DCSupplemental).

Published online May 28, 2019.

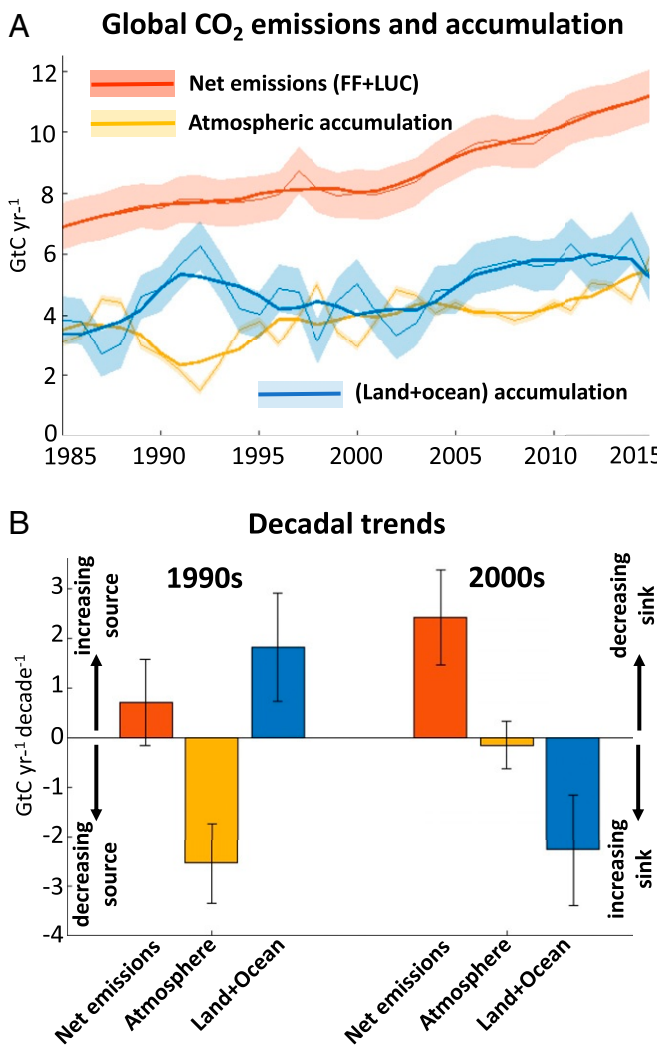


**Fig. 1.** (A) Global CO<sub>2</sub> emissions from fossil-fuel-burning, cement production, and land-use change (FF+LUC) (red curve), compared with the measured rate of accumulation of CO<sub>2</sub> in the atmosphere (gold curve) and the inferred rate of change of CO<sub>2</sub> accumulation in the land and ocean (blue curve). Thin lines are annual means, and thick lines are 5-y running means. (B) Decadal trends in CO<sub>2</sub> emissions (FF+LUC) and the atmospheric and total land+ocean sinks. For emissions, positive values indicate an increasing source and negative values a decreasing source (left-hand arrows; sign convention as in Eq. 1). For the atmosphere and land+ocean sinks, positive values indicate a decreasing sink and negative values an increasing sink (right-hand arrows; opposite the sign convention in Eq. 1). All data are from the 2017 Global Carbon Budget (3, 4). Error bars are  $1-\sigma$ .

(GOBMs) are often used to estimate the land and ocean carbon sinks, respectively (3). Methods have also been developed for estimating CO<sub>2</sub> accumulation in the ocean indirectly from observations using inverse models (10–12) and measurements of the sea-surface partial pressure of CO<sub>2</sub> (pCO<sub>2</sub>) (13–15).

While the terrestrial biosphere is the dominant source of interannual variability in the natural CO<sub>2</sub> sinks (5, 16), observations and numerical models have highlighted substantial decadal variability in ocean CO<sub>2</sub> uptake at both regional (17–19) and global scales (20, 21). In particular, recent estimates from several data-based models (22–24) suggest that the decadal variability in the ocean CO<sub>2</sub> sink is larger than currently estimated by global carbon budgets. To assess the robustness of decadal trends in ocean CO<sub>2</sub> uptake, here, we compare decadal variabil-

ity in the ocean carbon sink from three widely used independent methods: GOBMs participating in the 2017 Global Carbon Budget (3), an ocean circulation inverse model (OCIM) (12, 24), and pCO<sub>2</sub>-based flux mapping models from the Surface Ocean pCO<sub>2</sub> Mapping Intercomparison (SOCOM) project (15). We use these methods to deduce the contribution of the ocean carbon sink to the decadal variability of atmospheric carbon accumulation, to examine the mechanisms governing this variability, and to shed light on the decadal variability of the terrestrial CO<sub>2</sub> sink.

### Decadal Variability of the Ocean Carbon Sink

Estimates of the global ocean carbon sink from the GOBMs, SOCOM products, and the OCIM are in broad agreement regarding the magnitude and temporal evolution of ocean carbon accumulation over the past 30 y (Fig. 2A). Estimates of the ocean anthropogenic carbon sink in 2010 from these methods cluster around a mean of  $\sim 2.4$  GtC·y<sup>-1</sup> with an uncertainty of  $\sim 25\%$  due to differences among the various methods and models (Fig. 2A).

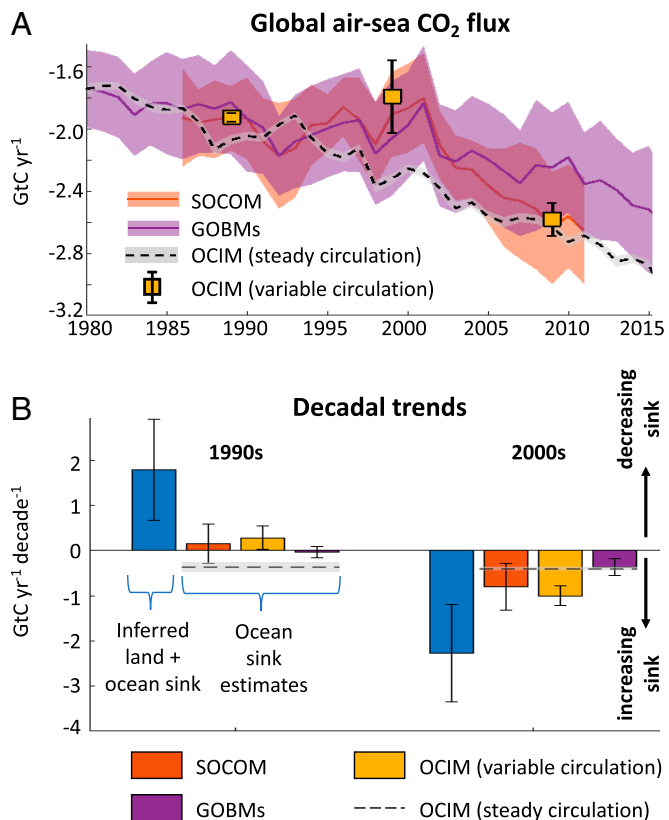


**Fig. 2.** (A) Estimates of the ocean carbon sink from a subset of models participating in the SOCOM project (15), a subset of GOBMs participating in the 2017 Global Carbon Budget (3) and an OCIM with (24) and without (12) decadal variability in ocean circulation. Thick lines are the ensemble mean from each method, with shading representing one SD uncertainty. For the OCIM with variable circulation, the mean value at the end of each decade (1989, 1999, and 2009) is shown, with error bars representing one SD. For the OCIM with constant circulation, error bars are the ensemble range. SOCOM results have been adjusted for outgassing of riverine CO<sub>2</sub> (*Materials and Methods*). (B) Decadal trends in the net (land+ocean) carbon sink (blue bar; same as in Fig. 1) and four estimates of decadal trends in the ocean carbon sink from SOCOM models (red bar), GOBMs (purple bar), and OCIM with decadal variability in ocean circulation (gold bar) and without any variability in ocean circulation (dashed line).

A closer look at the decadal trends in ocean CO<sub>2</sub> uptake reveals that the various methods of estimating the oceanic CO<sub>2</sub> sink differ in the magnitude of their decadal variability (Fig. 2B). The OCIM with steady circulation simulates CO<sub>2</sub> uptake by an ocean with no variability in circulation or biology (12), and therefore the decadal trends are very similar for both the 1990s and the 2000s, with global ocean CO<sub>2</sub> accumulation accelerating at  $\sim 0.4 \text{ GtC}\cdot\text{yr}^{-1}\cdot\text{decade}^{-1}$ . All of the other methods display significantly more decadal variability, strongly suggesting decadal trends in ocean circulation and/or biology over this time period (Fig. 2B).

Decadal trends in ocean CO<sub>2</sub> uptake are strongest in the observation-based models. In the 1990s, SOCOM products (15) and the OCIM with decadally varying circulation (24) diagnose a weakening trend of  $0.15 \pm 0.43$  and  $0.28 \pm 0.26 \text{ GtC}\cdot\text{yr}^{-1}\cdot\text{decade}^{-1}$ , respectively, which in turn accounts for 8% ( $-10\%$  to 83%) and 16% (1–77%) of the observed  $1.8 \pm 1.1 \text{ GtC}\cdot\text{yr}^{-1}\cdot\text{decade}^{-1}$  weakening of the net (land+ocean) carbon sink. In the 2000s, the SOCOM products estimate a strengthening of the ocean carbon sink by  $0.80 \pm 0.51 \text{ GtC}\cdot\text{yr}^{-1}\cdot\text{decade}^{-1}$  that is consistent with the  $1.0 \pm 0.2 \text{ GtC}\cdot\text{yr}^{-1}\cdot\text{decade}^{-1}$  strengthening inferred by the OCIM with variable circulation. These trends account for 35% (9–109%) and 43% (24–100%), respectively, of the observed  $2.3 \pm 1.1 \text{ GtC}\cdot\text{yr}^{-1}\cdot\text{decade}^{-1}$  strengthening trend of the total (land+ocean) carbon sink in the 2000s. Based on the average trends in the observation-based models over the 1990s and the first decade of the 2000s, the ocean is responsible for  $\sim 10\text{--}40\%$  of the observed decadal variability in the natural carbon sinks.

The GOBMs also simulate weaker-than-expected ocean CO<sub>2</sub> uptake during the 1990s followed by a strengthening trend during the 2000s, but the magnitude of decadal variability is smaller than that estimated by SOCOM and the variable-circulation OCIM. For example, in the 2000s, the growth rate of oceanic

CO<sub>2</sub> uptake in the GOBMs was slightly less than simulated by the OCIM with constant circulation and biology, while the other methods estimate that oceanic uptake was accelerating roughly twice as fast as it would with constant circulation and biology (Fig. 2B). According to average trends in the GOBMs over the 1990s and the first decade of the 2000s, the ocean is responsible for  $\sim 0\text{--}20\%$  of the decadal variability in the natural carbon sinks, which is about half of the variability estimated by the observation-based approaches.

Despite the overall agreement among the methods on the sign of the decadal variability in the ocean CO<sub>2</sub> sink, there is substantial spread in the magnitude of the decadal trends both across models within a particular method and across oceanographic regions (Fig. 3). With respect to the global ocean CO<sub>2</sub> uptake, the SOCOM products range from a trend of  $-0.21$  to  $1.11 \text{ GtC}\cdot\text{yr}^{-1}\cdot\text{decade}^{-1}$  in the 1990s to  $-0.21$  to  $-2.13 \text{ GtC}\cdot\text{yr}^{-1}\cdot\text{decade}^{-1}$  in the 2000s. Almost all (eight of nine) of the SOCOM products show a more rapidly strengthening CO<sub>2</sub> sink in the 2000s compared with the 1990s. Different GOBMs also exhibit substantially different decadal variability, although all of the GOBMs simulate a strengthening of the ocean CO<sub>2</sub> sink in the 2000s relative to the 1990s (Fig. 3A).

To examine regional patterns of decadal variability in the ocean CO<sub>2</sub> sink, we integrated the air-sea CO<sub>2</sub> fluxes within different regions based on biomes defined by ref. 25 (SI Appendix). The model-average trends across different methods (SOCOM, GOBMs, and OCIM), and in different oceanographic regions, display a remarkable pattern: In every region, every method (on average) predicts that the oceanic CO<sub>2</sub> uptake increased faster in the 2000s than in the 1990s (Fig. 3 B–F). The best agreement at regional scales across methods is found between the SOCOM products and the OCIM with variable circulation. In all regions, these methods infer an oceanic CO<sub>2</sub> sink that strengthened much faster in the 2000s than in the 1990s. In

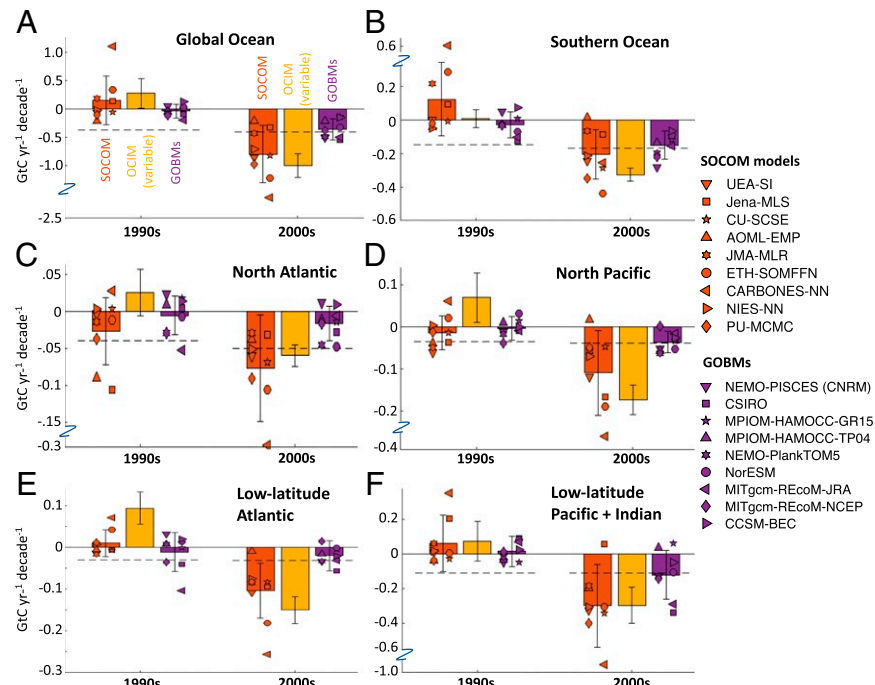


**Fig. 3.** Decadal trends in ocean carbon uptake for the global ocean (A) and for different ocean regions (B–F) as defined by the biomes of refs. 25 and 26 (see SI Appendix for biome definitions and definitions of the models used here). (B) Southern Ocean. (C) North Atlantic. (D) North Pacific. (E) Low-latitude Atlantic. (F) Low-latitude Pacific + Indian. The global ocean in A is the sum of the regions in B–F and does not include coastal regions and marginal seas. Trends and color-coding are as in Fig. 2B, with symbols representing individual models. Positive trends represent a weakening oceanic CO<sub>2</sub> sink and negative trends a strengthening oceanic CO<sub>2</sub> sink.

the high latitudes, the SOCOM-based estimates place more of the weakening in the 1990s CO<sub>2</sub> sink in the Southern Ocean, while the OCIM-based estimates suggest that more of the weakening occurred in the North Atlantic and North Pacific (Fig. 3 *B–D*). In the low latitudes, the SOCOM and OCIM models agree that the Pacific and Indian Oceans were a weakening sink in the 1990s (Fig. 3*F*), while the OCIM simulates a weaker-trending Atlantic Ocean sink than most of the SOCOM products (Fig. 3*E*). The strengthening of the ocean CO<sub>2</sub> sink in the 2000s is consistent across regions in both the SOCOM and OCIM models.

Decadal trends in the GOBM-simulated oceanic CO<sub>2</sub> uptake are not as variable as those diagnosed by the SOCOM products or the variable-circulation OCIM. For example, in the Southern Ocean, the observation-based methods infer large decadal variations in the ocean CO<sub>2</sub> sink, but the GOBMs simulate only a slight strengthening trend from the 1990s to the 2000s, with the exception of the NEMO-PISCES (CNRM) model, which simulates a large strengthening (Fig. 3*B*). The same is true in the low-latitude Pacific and Indian, which has the largest decadal variability next to the Southern Ocean in the observation-based estimates, but displays weak decadal variability in the GOBMs (Fig. 3*F*).

### Climate-Driven Trends in Ocean Carbon Uptake

To separate the impacts of CO<sub>2</sub>- and climate-forced variability on ocean CO<sub>2</sub> uptake in the GOBMs, we performed additional model simulations in which the climate forcing was held constant and in which the atmospheric CO<sub>2</sub> concentration was held constant (*Materials and Methods*). Based on these simulations, we isolated the decadal trends of oceanic CO<sub>2</sub> uptake due to atmospheric CO<sub>2</sub> increase and due to climate variability (Fig. 4). These simulations reveal that trends in ocean

CO<sub>2</sub> uptake in the 1990s and 2000s are nearly indistinguishable for the CO<sub>2</sub>-only forcing case (both between decades and among models) and that decadal variability in the CO<sub>2</sub> sink is driven exclusively by climate variability. Eight of nine of the GOBMs predict that climate variability drove a weakening of the global ocean CO<sub>2</sub> sink in the 1990s, and five of nine predict that climate variability drove a strengthening trend in the 2000s (Fig. 4*A*).

The regions with the strongest climate-driven decadal variability in the GOBMs are the Southern Ocean (Fig. 4*B*) and the low-latitude Pacific and Indian Oceans (Fig. 4*F*). Within these regions, however, the different models diverge substantially. In the Southern Ocean, the NEMO-PISCES (CNRM) model displays the largest climate-driven decadal variability, with decreasing CO<sub>2</sub> uptake in the 1990s and increasing CO<sub>2</sub> uptake in the 2000s, consistent with the observation-based estimates. But some models display the opposite trend, such as the CSIRO model, which simulates a weakening Southern Ocean CO<sub>2</sub> sink in the 2000s compared with the 1990s. In the low-latitude Pacific and Indian Oceans, it is the CSIRO model that displays the strongest climate-driven variability, in a direction consistent with the observation-based estimates.

Overall, climate variability drove a weakening of oceanic CO<sub>2</sub> uptake in the 1990s and a strengthening in the 2000s across multiple models and geographic regions. The geographical consistency of these trends suggests that this is a response to a global climatic pattern, likely large-scale changes in wind-driven ocean circulation (24, 27). These trends could be due to modes of internal variability in the climate system (22) or to external forcing [e.g., the eruption of Mount Pinatubo in 1991 (28, 29)], which can alter the states of internal climate modes (30), and thus the global winds. External drivers could be amplified by atmospheric (31) or oceanic (32) teleconnections to enhance decadal variability in ocean circulation.

Although the GOBMs display a consistent response to climate forcing, their climate-driven variability of ocean CO<sub>2</sub> uptake appears to be too weak compared with the data-based methods. Indeed, the GOBMs that perform best compared with the most accurate pCO<sub>2</sub>-based flux reconstructions are also the models that exhibit the largest decadal variability at the regional scale (*SI Appendix*, Figs. S1 and S2). The weak climate-forced variability of GOBMs might stem from either a weak ocean circulation response to atmospheric forcing or to changes in biologically driven carbon uptake that counteracts circulation-driven CO<sub>2</sub> uptake. To examine the latter possibility, we examined decadal trends in the biologically driven export of carbon below the surface ocean in the climate-forced GOBMs (*SI Appendix*, Fig. S3). Models with strong decadal variability in biological carbon export generally have weak decadal variability in climate-forced CO<sub>2</sub> uptake, while the opposite is true of models with weak variability in biological carbon export. Thus, the compensation between circulation-driven and biologically driven CO<sub>2</sub> uptake is one factor that reduces the sensitivity of the GOBMs to climate variability. The relative roles of biology and physics for determining decadal variability in ocean CO<sub>2</sub> uptake is poorly known and should be a priority for future study.

### Discussion and Conclusions

The agreement among the various methods of determining ocean CO<sub>2</sub> uptake demonstrates a broad consensus in the magnitude of the ocean carbon sink over the past several decades and in the timing of the decadal variability (Fig. 2). This agreement is especially encouraging, considering that the three methods considered here are entirely independent. The observation-based methods (SOCOM and OCIM) predict greater decadal variability of the ocean CO<sub>2</sub> sink than ocean biogeochemistry

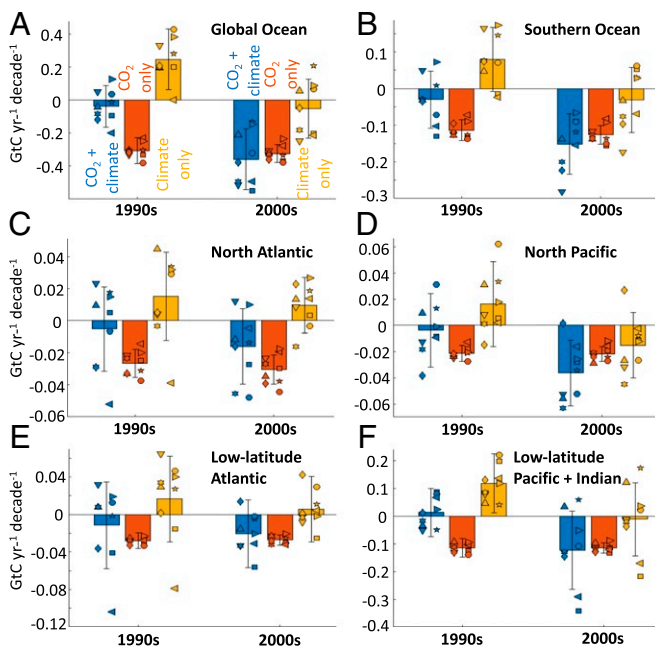


**Fig. 4.** Decadal trends in ocean carbon uptake simulated by GOBMs for the regions in Fig. 3. (A) Global ocean. (B) Southern Ocean. (C) North Atlantic. (D) North Pacific. (E) Low-latitude Atlantic. (F) Low-latitude Pacific + Indian. Shown separately are the trends due to both CO<sub>2</sub> and climate variability (blue bar; same as purple bar in Fig. 3), trends due to CO<sub>2</sub> variability only (red bar), and trends due to climate variability only (gold bar). Error bars are one SD of the model ensemble mean. Symbols represent results from individual models as defined in Fig. 3.

models and suggest that ~10–40% of the decadal variability in the natural CO<sub>2</sub> sinks can be attributed to the ocean. Ocean biogeochemistry models simulate less decadal variability of the ocean CO<sub>2</sub> sink, which could partly explain why current global carbon budgets (which rely mainly on GOBMs to estimate the oceanic CO<sub>2</sub> sink) have a declining budget imbalance in the 1990s, followed by an increasing imbalance in the 2000s (3). A muted variability of GOBMs compared with observations has also been observed for oxygen (33), suggesting that it is not unique to the carbon cycle.

These results also have important implications for decadal trends in the other major natural sink of anthropogenic CO<sub>2</sub>, the terrestrial biosphere. The decadal trends in the ocean CO<sub>2</sub> sink from the three methods considered here (SOCOM, OCIM, and GOBMs) can be compared with the total land+ocean CO<sub>2</sub> sink (Fig. 1B) to deduce the decadal trends in the terrestrial CO<sub>2</sub> sink (*Materials and Methods*). The decadal trends in the terrestrial CO<sub>2</sub> sink so calculated demonstrate that the terrestrial biosphere was a decreasing sink of CO<sub>2</sub> in the 1990s and an increasing sink of CO<sub>2</sub> in the first decade of the 2000s (the residual land sink in Fig. 5).

These decadal trends are in the same direction as those of the oceanic CO<sub>2</sub> sink, but even larger in magnitude, and can place important constraints on the DGVMs that are used to estimate the terrestrial CO<sub>2</sub> sink in the Global Carbon Budget (3). The DGVMs are in good agreement with the residual land sink regarding the strengthening of the terrestrial CO<sub>2</sub> sink in the 2000s, indicating consistency between the emissions data, the ocean CO<sub>2</sub> sink estimates, and the predictions of DGVMs during this period (Fig. 5). But during the 1990s, the DGVMs show less consistency, with one group of DGVMs simulating a neutral to weakening CO<sub>2</sub> sink (in agreement with the residual land sink) and another group simulating a strengthening CO<sub>2</sub> sink.

Differences between the residual land sink and the DGVM land sink during the 1990s could be due to biases in the ocean CO<sub>2</sub> sink estimates, in the CO<sub>2</sub> emissions, or in the DGVMs. Given the agreement between the three independent estimates

of the oceanic CO<sub>2</sub> sink, this is unlikely to be a source of bias. Errors in fossil-fuel CO<sub>2</sub> emissions (34) and LUC emissions (35) could be larger than reported and partly responsible for some of the discrepancy. The remaining discrepancies can be attributed to biases in the DGVMs, and as such could indicate a greater climate sensitivity of the terrestrial CO<sub>2</sub> sink than currently thought. In particular, the model discrepancies in the 1990s trends could partly reflect the different degrees to which the DGVMs are sensitive to the eruption of Mt. Pinatubo in 1991 (36) and the strong El Niño event of 1998 (16).

The findings of this study imply that both oceanic and terrestrial carbon-cycle models underestimate decadal variability in CO<sub>2</sub> uptake, which hinders the ability of these models to predict climate change on decadal timescales and likely contributes to decadal imbalances in current global carbon budgets (37). As the community moves toward decadal climate prediction (38, 39), it will be important to correctly resolve the climate sensitivity of oceanic and terrestrial carbon uptake. Continued development of observation-based methods for tracking ocean CO<sub>2</sub> uptake should alleviate their remaining structural errors (*SI Appendix*), leading to improved constraints on the magnitude and variability of the ocean CO<sub>2</sub> sink and reducing imbalances in global carbon budgets (37). This in turn will facilitate calibration of ocean biogeochemical models and terrestrial dynamic vegetation models, leading to improved climate projections and decadal predictions.

## Materials and Methods

**pCO<sub>2</sub>-Based Flux Mapping Products.** The SOCOM products are based on historical observations of surface-ocean pCO<sub>2</sub> compiled in the Surface Ocean CO<sub>2</sub> Atlas (SOCAT) (40) and the Lamont-Doherty Earth Observatory (41) datasets. The SOCOM models use various interpolation schemes to fill in the gaps in the data records to create continuous maps of pCO<sub>2</sub> at monthly resolution, from which air-sea fluxes are calculated (15). See *SI Appendix* for additional information.

**Inverse Models.** We use two versions of the OCIM. The first diagnoses the uptake of anthropogenic CO<sub>2</sub> in the absence of any changes to ocean circulation, solubility, or biology (12). Uncertainties are derived from the 10 different versions of the model described in ref. 12. The second version of the OCIM diagnoses the decadal-mean ocean CO<sub>2</sub> sink given decadal variations in ocean circulation along with mean state biology (24). Uncertainties are derived from 160 different versions of the model described in ref. 24. See *SI Appendix* for additional information.

**GOBMs.** We use a subset of the GOBMs used in the 2017 Global Carbon Budget (3): NEMO-PISCES (CNRM), CSIRO, NorESM, MPIOM-HAMOCC, NEMO-PlankTOM5, MITgcm-RECoM2, and CCSM-BEC. Each model performs three simulations: Simulation A uses reanalysis climate forcing and observed atmospheric CO<sub>2</sub> concentrations from 1959–2017. Simulation B uses constant climate forcing and atmospheric CO<sub>2</sub>. Simulation C uses constant climate forcing and observed atmospheric CO<sub>2</sub> concentrations from 1959–2017. In Fig. 4, “CO<sub>2</sub>+climate” is from simulation A, “CO<sub>2</sub> only” is from simulation C-simulation B, and “climate only” is from simulation A-simulation C. Models differ in their spin-up procedure and climate forcing, as detailed in *SI Appendix* and *SI Appendix*, Table S1.

**Accounting for Riverine Carbon.** The OCIM and GOBMs do not account for a degassing of 0.45–0.78 GtC·y<sup>-1</sup> (42, 43) of riverine CO<sub>2</sub>, but the SOCOM products do. To make the CO<sub>2</sub> fluxes comparable across all methods, we add a flux of 0.6 GtC·y<sup>-1</sup> to the globally integrated SOCOM CO<sub>2</sub> sink in Fig. 2.

**Calculating Decadal Trends.** Air-sea CO<sub>2</sub> fluxes from the SOCOM products, the GOBMs, and the steady-circulation OCIM are annually averaged, then used to compute the linear trend in ocean CO<sub>2</sub> uptake for the 1990s (1990–1999) and the first decade of the 2000s (2000–2009). Uncertainties on the decadal trends for each method include ensemble uncertainty, as well as an uncertainty of  $\pm 1$  y for the beginning and ending years of the trend calculations (i.e., 1990  $\pm 1$  to 1999  $\pm 1$  and 2000  $\pm 1$  to 2009  $\pm 1$ ). For the variable-circulation OCIM, decadal trends are calculated as the average air-sea flux within a given decade minus the average

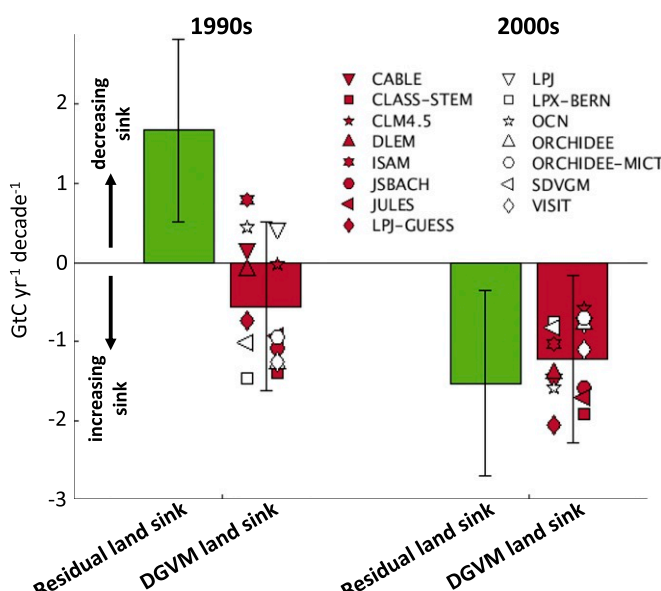


**Fig. 5.** Trends in the terrestrial CO<sub>2</sub> sink calculated as a residual from the global carbon budget (Eq. 1) using the estimates of the ocean CO<sub>2</sub> sink from three methods considered here (GOBMs, SOCOM, and OCIM with variable circulation) and from the DGVMs participating in the 2017 Global Carbon Budget (3). See *SI Appendix* for definitions of DGVMs used here.

air-sea flux in the preceding decade. This method minimizes the effects of discontinuities in the air-sea CO<sub>2</sub> flux introduced by abrupt changes in the ocean circulation at the demarcations of different decades (1990 and 2000) and gives trends similar to those using the final year of each decade (i.e., 2009–1999) to calculate trends. For regional decadal trends in Figs. 3 and 4, we integrate the air-sea CO<sub>2</sub> fluxes over distinct oceanographic regions based on the time-mean open-ocean biomes defined by ref. 25. To avoid differences in the model domains near the coast, the global ocean CO<sub>2</sub> uptake in all figures is the summation over all of the individual open-ocean regions and thus ignores a small contribution from coastal regions as well as the polar ice-covered regions. See *SI Appendix* for more information.

**Calculation of Decadal Trends in the Terrestrial CO<sub>2</sub> Sink.** To calculate decadal trends in the terrestrial CO<sub>2</sub> sink, we first calculate decadal trends in the ocean carbon sink using all of the methods considered here that resolve decadal variability in the ocean CO<sub>2</sub> sink (SOCOM, GOBMs, and OCIM-variable, as displayed in Fig. 2B). We then subtract these ocean-only trends from the trend in the total (land+ocean) CO<sub>2</sub> sink (Fig. 1B) to obtain the trends in the “residual land sink” (Fig. 5). Reported uncertainties include uncertainty in the CO<sub>2</sub> emissions, uncertainty in the atmospheric CO<sub>2</sub> concentration, uncertainty in the ocean CO<sub>2</sub> sink (treating all methods of estimating the ocean CO<sub>2</sub> sink as equally probable), and uncertainty due to varying the beginning and ending years for the trend calculation by ±1 y. Trends in the terrestrial CO<sub>2</sub> sink in the DGVMs are calculated in exactly the same way as those for the GOBMs, varying the starting and ending points

of the trend calculation for each DGVM by ±1 y. See *SI Appendix* for a full list of the DGVMs used here.

## Data Availability.

OCIM data are available at <https://tdevries.eri.ucsb.edu/models-and-data-products/>. Timeseries of the SOCOM data following ref. 15 can be obtained from <http://www.bgc-jena.mpg.de/SOCOM/>. Timeseries of the GOBM data are available at <https://doi.org/10.6084/m9.figshare.8091161>.

**ACKNOWLEDGMENTS.** We thank Rebecca Wright and Erik Buitenhuis at University of East Anglia, Norwich, for providing updated runs from the NEMO-PlankTOM5 model. T.D. was supported by NSF Grant OCE-1658392. C.L.Q. thanks the UK Natural Environment Research Council for supporting the SONATA Project (Grant NE/P021417/1). P.L. was supported by the Max Planck Society for the Advancement of Science. J.H. was supported under Helmholtz Young Investigator Group Marine Carbon and Ecosystem Feedbacks in the Earth System (MarEsSys) Grant VH-NG-1301. S.B. and R.S. were supported by the H2020 project CRESCENDO “Coordinated Research in Earth Systems and Climate: Experiments, Knowledge, Dissemination and Outreach,” which received funding from the European Union’s Horizon 2020 research and innovation program under Grant No 641816. SOCAT is an international effort, endorsed by the International Ocean Carbon Coordination Project, the Surface Ocean-Lower Atmosphere Study, and the Integrated Marine Biosphere Research program, to deliver a uniformly quality-controlled surface ocean CO<sub>2</sub> database. The many researchers and funding agencies responsible for the collection of data and quality control are thanked for their contributions to SOCAT.

1. G. Myhre et al., Anthropogenic and Natural Radiative Forcing, Stocker T, et al., Eds. (Cambridge Univ Press, Cambridge, UK, 2013), pp. 659–740.
2. P. Ciais et al., Carbon and Other Biogeochemical Cycles, Stocker T, et al., Eds. (Cambridge Univ Press, Cambridge, UK, 2013), pp. 465–570.
3. C. Le Quéré et al., Global carbon budget 2017. *Earth Syst. Sci. Data*, 10, 405–448 (2018).
4. C. Le Quéré et al., Supplemental data of Global Carbon Budget 2017 (Version 1.0) [Data set]. Global Carbon Project. <https://doi.org/10.18160/gcp-2017>. Accessed 7 May 2019.
5. T. F. Keenan et al., Recent pause in the growth rate of atmospheric CO<sub>2</sub> due to enhanced terrestrial carbon uptake. *Nat. Commun.*, 7, 13428 (2016).
6. M. R. Burton, G. M. Sawyer, D. Granieri, Deep carbon emissions from volcanoes. *Rev. Mineralogy Geochem.*, 75, 323–354 (2013).
7. R. J. Andres, T. A. Boden, D. Higdon, A new evaluation of the uncertainty associated with CDIAC estimates of fossil fuel carbon dioxide emission. *Tellus B*, 66, 23616 (2014).
8. A. Ballantyne et al., Audit of the global carbon budget: Estimate errors and their impact on uptake uncertainty. *Biogeosciences*, 12, 2565–2584 (2015).
9. T. J. Conway et al., Evidence for interannual variability of the carbon cycle from the National Oceanic and Atmospheric Administration/Climate Monitoring and Diagnostics Laboratory Global Air Sampling Network. *J. Geophys. Res. Atmos.*, 99, 22831–22855 (1994).
10. N. Gruber et al., Oceanic sources, sinks, and transport of atmospheric CO<sub>2</sub>. *Glob. Biogeochem. Cycles*, 23, GB1005 (2009).
11. S. Khatiwala, F. Primeau, T. Hall, Reconstruction of the history of anthropogenic CO<sub>2</sub> concentrations in the ocean. *Nature*, 462, 346 (2009).
12. T. DeVries, The oceanic anthropogenic CO<sub>2</sub> sink: Storage, air-sea fluxes, and transports over the industrial era. *Glob. Biogeochem. Cycles*, 28, 631–647 (2014).
13. T. Takahashi et al., Climatological mean and decadal change in surface ocean pCO<sub>2</sub>, and net sea-air CO<sub>2</sub> flux over the global oceans. *Deep Sea Res. Part II*, 56, 554–577 (2009).
14. P. Landschützer, N. Gruber, D. Bakker, U. Schuster, Recent variability of the global ocean carbon sink. *Glob. Biogeochem. Cycles*, 28, 927–949 (2014).
15. C. Rödenbeck et al., Data-based estimates of the ocean carbon sink variability—first results of the surface ocean pCO<sub>2</sub> mapping intercomparison (SOCOM). *Biogeosciences*, 12, 7251–7278 (2015).
16. J. S. Kim, J. S. Kug, J. H. Yoon, S. J. Jeong, Increased atmospheric CO<sub>2</sub> growth rate during El Niño driven by reduced terrestrial productivity in the CMIP5 ESMs. *J. Clim.*, 29, 8783–8805 (2016).
17. T. Takahashi, S. C. Sutherland, R. A. Feely, C. E. Cosca, Decadal variation of the surface water PCO<sub>2</sub> in the western and central equatorial Pacific. *Science*, 302, 852–856 (2003).
18. P. Landschützer et al., The reinvigoration of the southern ocean carbon sink. *Science*, 349, 1221–1224 (2015).
19. M. L. Breeden, G. A. McKinley, Climate impacts on multidecadal pCO<sub>2</sub> variability in the North Atlantic: 1948–2009. *Biogeosciences*, 13, 3387–3396 (2016).
20. A. Fay, G. McKinley, Global trends in surface ocean pCO<sub>2</sub> from in situ data. *Glob. Biogeochem. Cycles*, 27, 541–557 (2013).
21. R. Séférian, S. Berthet, M. Chevallier, Assessing the decadal predictability of land and ocean carbon uptake. *Geophys. Res. Lett.*, 45, 2455–2466 (2018).
22. P. Landschützer, N. Gruber, D. C. Bakker, Decadal variations and trends of the global ocean carbon sink. *Glob. Biogeochem. Cycles*, 30, 1396–1417 (2016).
23. P. Landschützer, T. Ilyina, N. S. Lovenduski, Detecting regional modes of variability in observation-based surface ocean pCO<sub>2</sub>. *Geophys. Res. Lett.*, 46, 2670–2679 (2019).
24. T. DeVries, M. Holzer, F. Primeau, Recent increase in oceanic carbon uptake driven by weaker upper-ocean overturning. *Nature* 542, 215–218 (2017).
25. A. Fay, G. McKinley, Global open-ocean biomes: Mean and temporal variability. *Earth Syst. Sci. Data*, 6, 273–284 (2014).
26. A. Fay, G. McKinley, Global ocean biomes: Mean and time-varying maps (NetCDF 7.8 MB). PANGAEA. <https://doi.org/10.1594/PANGAEA.828650>. Accessed 7 May 2019.
27. C. Le Quéré, T. Takahashi, E. T. Buitenhuis, C. Rödenbeck, S. C. Sutherland, Impact of climate change and variability on the global oceanic sink of CO<sub>2</sub>. *Glob. Biogeochem. Cycles*, 24, GB4007 (2010).
28. T. Frölicher, F. Joos, C. Raible, Sensitivity of atmospheric CO<sub>2</sub> and climate to explosive volcanic eruptions. *Biogeosciences*, 8, 2317–2339 (2011).
29. M. R. Raupach et al., The declining uptake rate of atmospheric CO<sub>2</sub> by land and ocean sinks. *Biogeosciences*, 11, 3453–3475 (2014).
30. S. Stevenson et al., Climate variability, volcanic forcing, and last millennium hydroclimate extremes. *J. Clim.*, 31, 4309–4327 (2018).
31. S. McGregor, M. F. Stuecker, J. B. Kajtar, M. H. England, M. Collins, Model tropical Atlantic biases underpin diminished Pacific decadal variability. *Nat. Clim. Change*, 8, 493–498 (2018).
32. R. G. Peterson, W. B. White, Slow oceanic teleconnections linking the Antarctic Circumpolar Wave with the tropical El Niño-Southern Oscillation. *J. Geophys. Res. Oceans*, 103, 24573–24583 (1998).
33. O. Andrews, N. Bindoff, P. Halloran, T. Ilyina, C. Le Quéré, Detecting an external influence on recent changes in oceanic oxygen using an optimal fingerprinting method. *Biogeosciences*, 10, 1799–1813 (2013).
34. T. Saeki, P. Patra, Implications of overestimated anthropogenic CO<sub>2</sub> emissions on East Asian and global land CO<sub>2</sub> flux inversion. *Geosci. Lett.*, 4, 9 (2017).
35. C. Le Quéré et al., Trends in the sources and sinks of carbon dioxide. *Nat. Geosci.*, 2, 831 (2009).
36. T. L. Frölicher, F. Joos, C. C. Raible, J. L. Sarmiento, Atmospheric CO<sub>2</sub> response to volcanic eruptions: The role of ENSO, season, and variability. *Glob. Biogeochem. Cycles*, 27, 239–251 (2013).
37. C. L. Quéré et al., Global carbon budget 2018. *Earth Syst. Sci. Data*, 10, 2141–2194 (2018).
38. G. J. Boer et al., The decadal climate prediction project (CDPP) contribution to CMIP6. *Geosci. Model Dev.*, 9, 3751–3777 (2016).
39. S. Yeager et al., Predicting near-term changes in the earth system: A large ensemble of initialized decadal prediction simulations using the community earth system model. *Bull. Am. Meteorol. Soc.*, 99, 1867–1886 (2018).
40. D. C. E. Bakker et al., A multi-decade record of high-quality fCO<sub>2</sub> data in version 3 of the Surface Ocean CO<sub>2</sub> Atlas (SOCAT). *Earth Syst. Sci. Data*, 8, 383–413 (2016).
41. T. Takahashi, S. C. Sutherland, A. Kozyr, *Global Ocean Surface Water Partial Pressure of CO<sub>2</sub> Database: Measurements Performed during 1957–2013* (National Oceanographic and Atmospheric Administration, Silver Spring, MD, Version 2013, 2014).
42. A. R. Jacobson, S. E. Mikaloff Fletcher, N. Gruber, J. L. Sarmiento, M. Gloo, A joint atmosphere-ocean inversion for surface fluxes of carbon dioxide: 1. Methods and global-scale fluxes. *Glob. Biogeochem. Cycles*, 21, GB1019 (2007). Correction in: *Glob. Biogeochem. Cycles*, 21, GB2025 (2007).
43. L. Resplandy et al., Revision of global carbon fluxes based on a reassessment of oceanic and riverine carbon transport. *Nat. Geosci.*, 11, 504–509 (2018).